Drones for Inspection of Overhead Power Lines with Recharge Function

Conference Paper · August 2020

DOI: 10.1109/DSD51259.2020.00084

5 authors, including:

Emad Samuel Malki Ebeid
University of Southern Denmark
79 PUBLICATIONS **872** CITATIONS

SEE PROFILE

Andreas Hennig
Hochschule Ruhr West
27 PUBLICATIONS **93** CITATIONS

SEE PROFILE

Drones for Inspection of Overhead Power Lines with Recharge Function

Authors

***Abstract*—In recent years drones have proven their ability to solve complex tasks autonomously and effectively. Drones have not been present as a ubiquitous technology for solving these tasks yet. The reason is mainly due to their limited flying time. The technology has great market potential in many areas if flight time could be increased. However, only a few solutions for recharging are available, but none for recharging on power lines. This remains a research topic for now. Through this paper a novel energy harvesting design is presented based on inductive coupling, allowing a drone to grasp and perch onto an overhead power line to recharge its batteries. The overall electronic design was based on analyzing and simulating different current transformers in simulation before testing in the laboratory. The split-core including windings was integrated into a gripping mechanism, verified by analytical and numerical analysis as well as non-destructive and destructive testing. The results indicate that enough power can be harvested from the powerline to recharge the drone batteries. The theoretically achievable power was also found to be within the expected range. With this design, drones can solve time-consuming and complex tasks in the future.**

Keywords— Energy harvesting, Energy self-sufficient drones, Inductive harvesting, MPP-tracking, Infrastructure inspection

I. INTRODUCTION

The use of drones is increasingly gaining interest for labor-intensive tasks such as infrastructure inspection. Up to now, drones have limited energy resources and computing power, which particularly limits functions based on long-term operations. To meet these challenges, which result from the limited resources of the drone, a new architecture is proposed, which on the one hand provides for networking with other drones and the cloud, and on the other hand, allows recharging of batteries from overhead lines. In the research project "Drones4Energy" [1], these ideas for a new type of drone platform are being implemented for the first time and tested using the example of overhead line inspection [2].

The overall objective of the Drones4Energy project is to be able to monitor overhead lines in the future in a cost-effective and automated manner. Cameras and LiDAR sensors on the drones record the components of the system such as the conductor cable, insulator and tower. Machine learning and artificial intelligence enable autonomous operation and synchronization with other drones in a swarm. This eliminates the need for costly and dangerous helicopter flights for infrastructure monitoring.

The project intents to deliver a collaborative drone system that can inspect the power grid in a highly efficient manner by allowing a swarm of drones to fly autonomously along the power lines rather than individual drones (Figure 1).

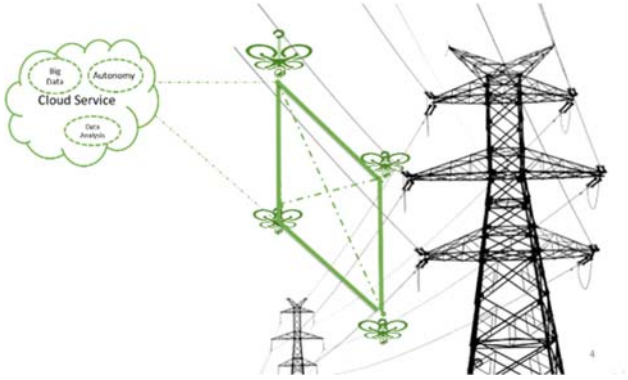

Figure 1 Principle of the inspection of overhead lines by swarms of drones

A. Networking of drones for the inspection process

In order to optimize inspection time and improve accuracy, a collaborative drone system will be formed that flies along both sides of the overhead line. A hybrid, low-power, long-range wireless communication network based on both LoRaWAN technology and broadband cellular network mechanisms are being developed by project partner Develco A/S. The network will enable inter-drone communication together with Internet communication to monitor and control the drones via the ground control station. In this way, the drones' missions will be updated and inspection results collected [3].

B. Energy Harvesting

A special requirement is to achieve the longest possible flight time in order to be able to use the autonomous operation efficiently. Since increasing the battery capacity will result in added weight, the conductor rope was intended to serve as an energy source. Through an inductive harvester the drone can be recharged. The drone perches on the overhead line with the harvester and charges the drone's battery. This limits the weight, but significantly extends the flight time and thus the operating time.

Based on an inductive coupling, a harvester for the drone is developed. The concept is based on a clip-on converter whose core closes around the rope when the drone docks with the high-voltage rope (Figure 2).

In contrast to the supply of sensor nodes, the harvester should provide a power supply that is preferably in the high-power range up to about 100 watts, whereby the weight of the core and the winding must be as low as possible for the reasons mentioned above. Up to now, designs with off-the-shelf cores have been realized for test measurement at the low current levels in the conductor cables of 100 to 380 A. Customized cores, in which shape and material are adapted to the application, are expected to provide even higher power yields in the future.

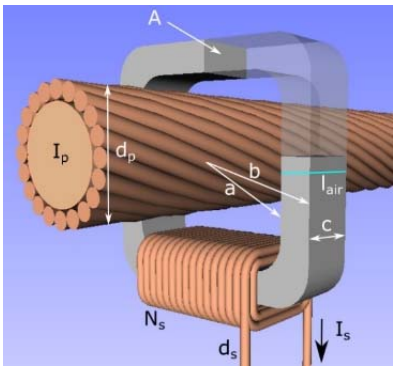

Figure 2 Principle of energy harvester with clip-on converter core and conductor rope

C. Docking to the overhead line

A state-of-the-art drone platform is being developed by the University of Southern Denmark (SDU). To stabilize the drone near a live conductor rope, navigate the harvester to the rope and at the same time be immune to magnetic interference. A combination of precision navigation systems, LiDAR systems, and magnetic sensors is built into the drone. The control system analyses the acquired data, plans the approach to the conductor, considering e.g. the inclination of the rope and wind, and then performs the safe docking (Figure 3). When the battery is full, the drones have synchronized in the swarm and the weather permits flight, the control system performs the safe takeoff and releases the cable.

Figure 3 Drone with docking mechanism

II. State of the Art

Energy Harvesting is a key component of the sustainable solution for the energy supply of mobile devices and the realization of autonomous sensor systems. Two lines have emerged in the development of contactless power transmission. Under the term WPT - Wireless Power Transfer, solutions are found that can transmit high power without contact. In special solutions, the power ranges up to 1 kW or even higher [4] [5]. Examples can be found in the battery charging of e-scooters and e-cars. Research is also being conducted on special charging systems of this type for drones [6]. Here, the focus is on landing sites that can be approached by drones. These stations can be located on buildings or lamp posts, for example.

These approaches also use an inductively coupled transmission path. However, both primary and secondary sides are subject to be optimized. When docking to the overhead line, the primary side is reduced to the conductor rope and represents the worst conceivable starting position for the transmission link (Figure 2). Therefore, these approaches cannot be used for the charging concept of the drone's battery.

The second line refers to energy harvesting for the supply of IoT devices. Here, autonomous sensors are considered which collect process data independent of cable and battery and forward them via wireless communication to an edge server or cloud server. Typical examples are retrofit sensors in industrial plants for the analysis of power consumption of machines or smart grid sensors for power monitoring in distribution networks [7]. The energy requirement of these IoT modules is of the order of a few 100 milliwatts at most [8].

In contrast to these solutions, this paper presents an extended approach to investigate energy harvesting for battery charging in drones from overhead lines. With this new approach, no additional infrastructure needs to be provided. However, the boundary conditions with the high required power and changing conditions are a challenge that has not yet been solved. Within the Drones4Energy project, the feasibility is being investigated.

III. Design Aspects of the Harvester

A. Objectives and requirements

In order to find a workable solution that is suitable for practical use, numerous requirements have to be met, here are some essential points:

The drone must be able to dock independently to the line. In addition to good algorithms for controlling the flight path, this requires high-precision sensors for local navigation in the detection of the cables and their approach under the influence of disturbance variables such as wind. High electrical and magnetic fields occur in the vicinity of the cable, and displacement or compensating currents can also flow at the first touch to the cable. The drone must have a high immunity to these influences. After closing the core around the conductor rope, the drone can go into sleep mode and the battery can be charged. The closing mechanism should clamp the drone firmly to the rope.

The harvester must be made of a specific core material and have a copper winding. Due to the high power requirement for charging the batteries, these parts require a considerable weight, which results from a large cross-section of core and wire. In the design, special attention should therefore be paid to keeping the weight as low as possible. This can be influenced by shaping the core, optimizing the winding and wire. For performance considerations, the quotient of achievable power divided by weight will be introduced later to allow designs to be compared.

B. Specification

The following specifications of essential parameters and operating conditions of Table 1 were considered during development.

Table 1: Specifications and operating conditions

Ambient Conditions	
Ambient temperature	5 °C to 45 °C
Typical overhead line diameters	25 mm to 45 mm
Range of overhead line current	200 A to 1500 A
Average overhead line current	400 A to 600 A
Electrical Parameters	
Cell voltage	3.7 V (nominal) / 4.1 V (max.)
Charging current	3 to 10 A (1C max.)
Number of cells	up to 6

As can be seen from the specification, the operation is assumed to take place under suitable climatic conditions. Primarily addressed are overhead lines of the medium and high voltage level and transport and distribution networks.
The rechargeable battery is built from standard 3.7 V Li-cells in combined parallel and series connection, e.g. six cells in series connection represent a nominal voltage of 22.2 V.

C. *Mechanical considerations*

As explained in A, a mechanism to achieve a perching state for the drone was critical. An initial constraint to use the GMC SC-50E split-core current transformer was set for developing the first mechanism prototype. For safety reasons, it was determined to approach the lowest conductor available and let the drone perch from below. It is of great importance to have a mechanism with a failsafe function to minimize the chance of a drone stuck on the cable in case of failure. The mechanism was furthermore lifted to a safe distance from the propeller to not crash with the conductor. This has been further explained in section IV.C.

IV. HARVESTER DEVICE

A. *Calculation of maximum achievable power*

First, the energy transfer is derived analytically. From the basic electrotechnical equations, the theoretical maximum power is determined as a function of the current in the conductor rope and a simulation model is created. In simulations the significant parameters are varied and the behavior of the energy transfer is analyzed. From this essential influencing parameters are identified and taken into account for later optimization.

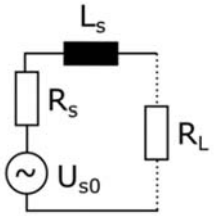

Figure 4 Equivalent circuit on the secondary side of the transformer

According to the rules of power matching, the load resistance should be adapted to the internal impedance. For this purpose, the components of the transformer are determined based on the equivalent circuit. The assumed equivalent circuit on the secondary side is shown in Figure 4.

As described above (Sec.I.B), the method of inductive coupling with a current transformer is used for energy harvesting. A core is placed around the conductor rope, on which the secondary winding is located (Figure 2). The primary winding, in this case, consists only of the conductor rope which is passed through the core, this could be assumed as a winding with less than one turn. Therefore, the classical transformer equation can only be applied inadequately. For the calculation, however, the induction law is applied instead of the transformer equation. First, the magnetic flux in the core is calculated, and from this the induced voltage at the secondary coil.

To calculate the induced voltage U_{s0}, the well-known equations are formed to equation (4):

(1) Magnetic field strength as a function of the distance to the conductor,
(2) Magnetic flux density and
(3) Magnetic flux as integral of the magnetic flux density over the area of interest.

$$H(r) = \frac{I_p}{2*\pi*r} \qquad (1)$$

$$B(r) = \mu_0 * \mu_{r,core} * H(r) \qquad (2)$$

$$\Phi = \iint_A \vec{B} d\vec{A} \qquad (3)$$

To solve the integral in equation (3), it is assumed for simplicity that a toroid-shaped core and coil is used and the core has a rectangular cross-section. Table 2 shows the used parameters. Then the surface integral runs over the radius from inner radius ‘a’ to outer radius ‘b’ and over the length ‘c’.

$$U_{s0} = \frac{d\Phi}{dt} = \frac{\omega}{2\pi} * \mu_0 * \mu_r * N_s * c * ln\left(\frac{b}{a}\right) * I_p \qquad (4)$$

Table 2: Parameters of the transformer

	Parameter	Associated parameters/notes
I_p	Primary Current Average or minimum current defines working point of harvester	d_p diameter of high voltage line I_p sc short circuit current t_Ipsc time of short circuit current I_p_max maximum continuous I_p I_p_min minimum I_p
fc	Net frequency	typ. 50 Hz
a b c	Core dimensions	a inner spacing/radius of core b outer dimension c length of core
l_air	Length of air gap	Reduces effecitive permeability of the core (sheares hysteresis)
μ_r	Permeability of core material	Hc Coercivity Br Remanence Bsat Saturation
Ns	Number of turns of secondary winding (limited by wire diameter and core dimensions)	ds diameter of copper wire of Secondary winding (limits continuous primary current)
I_s	Secondary current	U_s0 no-load induction voltage I_s = I_p/N_s (worst case)

In the same way, the inductance Ls of the secondary winding can be derived from equation (4) into equation (5):

$$L_s = \frac{1}{2\pi} * \mu_0 * \mu_r * N_s{}^2 * c * ln\left(\frac{b}{a}\right) \qquad (5)$$

Together with the angular frequency ‘ω’, Inductance ‘L_s’ and the DC resistance ‘R_s’ the impedance ‘Z_s’ can be calculated in equation (6) and used in equation (7) for the determination of the maximum available power for battery charging.

$$Z_s = R_s + j\omega L_s \qquad (6)$$

$$P_{RL} = U_{s0}{}^2 * \frac{R_L}{(Z_s+R_L)*(Z_s{}^*+R_L)} \qquad (7)$$

A special feature is the use of a clip-on core. An air gap must be taken into account for this. In the calculation, this is reflected in the permeability. In the flux density (2) an effective permeability ‘$\mu_{r,eff}$’ is used instead of the relative permeability ‘μr’ and calculated according to equation (9). Here, the magnetic length ‘μ_{mag}’ of the core is related to the sum of core length and air gap length ‘μ_{air}’.

$$\mu_{r,eff} = \mu_r * \frac{l_{mag}}{l_{mag}+l_{air}*\mu_r} \qquad (8)$$

From this approach, a simulation model was developed to support the design of an energy harvesting module. The following figures show the maximum achievable power P_{MPP} as a function of the current in the conductor ‘I_p’ (Figure 5) and the power at the load resistance PRL as a function of the load resistance (Figure 6) in a qualitative representation. The magnetic core has an inner diameter of 50.5 mm and a core cross-section of 6 mm to 20 mm.

The model considers in equation (6) the inductance L_s as constant and neglects losses in the core material of the transformer and the wire of the secondary winding ($R_s << \omega L_s$). Furthermore, the load is seen as a pure ohmic resistance.

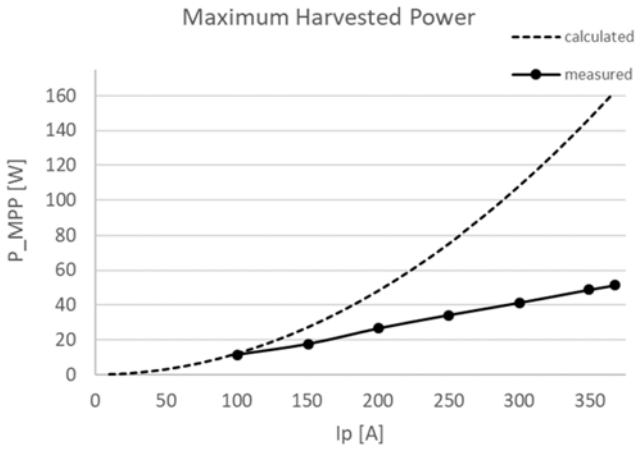

Figure 5 Simulation result of maximum power vs. primary current

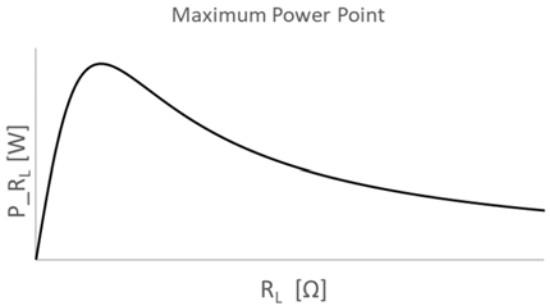

Figure 6 Simulation result of maximum power vs. load resistance

The dashed curve in Figure 5 shows the maximum achievable power calculated from the model. It shows the typical square increase. The simulation results show, that already below the specified average primary current the theoretically achievable power is within the expected and useful range.

Further investigations have shown that the number of windings has only a marginal influence on the achievable output. Thus, an adaptation to the desired output voltage can easily be made.

Moreover, Figure 6 shows the dependence of the maximum achievable power on the value of the load resistance. An automatic adjustment of the load resistance must be implemented in the subsequent electronics in order to always work at the point of optimal power transmission.

B. Measuring results

A laboratory setup, as shown in Figure 7, is used to verify the results. The challenge is to provide the high primary current, which is usually only available in high current laboratories. Instead of the single conductor, a conductor loop with several windings was implemented for the primary side, with N_p: number of turns of the primary side.

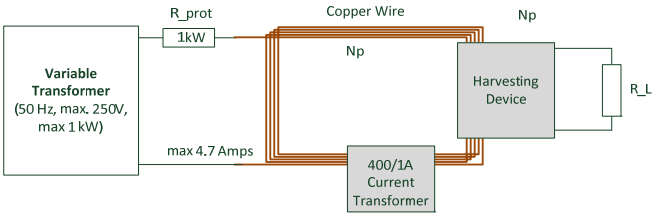

Figure 7 Test setup for transformer evaluation and measurement of maximum achievable power

The conductor loop is fed from an adjustable source with a series-connected protective resistor R_{prot}, allowing equivalent primary currents of up to 380 A to be generated. The source and protective resistor must be able to withstand powers of up to 1 kW.

Suitable test samples as off-the-shelf components of magnetic cores were selected for the investigation. The criteria used were the relative permeability of the core material μ_r, the

loss factor of the core material tanδ, and the geometry. Table 3 shows some properties of the selected samples.

With the support of the simulation tool, the winding was designed. 400 turns are provided for both cores. The wire cross-section is chosen so large that the resistance R_3 in equation (6) only takes up a few ohms and can be neglected compared to the reactance ωL_3. A cascade of power resistors is used as a load.

Table 3: Test samples of transformer cores


Type	GMC SC50-E	MLX9
Core material	Silicon iron?	electrical steel
Core Properties	High saturation flux density Medium losses	High saturation flux density, Low losses, large geometry
Mass of core	194 g	700 g
Power @ 380A	16 W	51 W
Manufacturer	*www.gmc-instruments.de*	*www.waasner.de*

The representation of the measured values in Figure 5 refers to the transformer with the MLX9 core. It can be seen immediately that the measured power changes from about a primary current of about 100 A into a linear function which shows a much lower output than the calculated output. At 350 A the measured value is about one-third of the theoretically achievable value. The model of the calculated function does not yet correspond to the actual behavior. To discuss the results, the possible causal effects are listed, these are saturation in the core, losses in the core, losses in the winding, and the relative permeability of the core material.

- The **saturation** results from a hysteresis during remagnetization. This applies to equation (2), the flux density does not reach the expected value afterward and also the induced voltage. It is assumed that the saturation is the main reason for the lower measured power.
- **Core losses** do occur, but both the indications from the manufacturer and the low observed warming suggest that core losses are very low.
- **Losses in the winding** can be easily determined by the dimensioning. Here, too, the low heat generation indicates low and negligible losses.
- Although the **relative permeability** is also strongly related to saturation, it can also vary additionally depending on the field strength. This can also cause a loss of power.

A strong dependence on the material is therefore evident. In order to increase the energy that can be extracted, it is necessary to further investigate how the material behaves at high field strengths and power levels. This behavior must be included in the model in order to obtain realistic results even for the typical conditions. It is also necessary to investigate whether materials are available which have a higher saturation field strength.

C. Mechanical gripper design

Based on the initial considerations from section II.-C the following design was determined, manufactured, and tested.

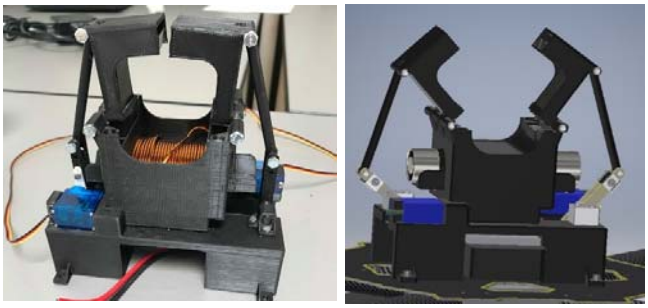

Figure 8 - Gripper CAD model and prototype

The upper part of the core has been separated into two equally sized pieces. A servo motor on each side operates the top parts from open to closed by rotating an arm and push the force through a strut. This lowers the center of gravity of the design. When the servomotor reaches the closed position, an electromagnet holds the arm and acts as the mechanism lock. The mechanism secures to an adapter which gains the required distance from the drone to the powerlines.

If the power of the drone would fail, the electromagnets release and the mechanism opens from the drone mass. It was further calculated and tested that the electromagnet minimum holding force to maintain a 3 kg drone was 27 N. The design was made to embed two Type 58 (0120) electromagnets [9] from SG transmission, with a holding force of 90 N, yielding a positive factor of safety above 3. Assuming a drone mass of 3 kg the moment translated and exerted to the servomotor shaft was determined by analytical methods as 0.38 Nm. Since tests revealed the servo release at 0.057 Nm, there was proof of sufficient load from the drone mass to release the mechanism, if the power to the electromagnet was cut. Lastly, the critical component of the break was determined by destructive testing to be the servo-arm. The break occurred at the pinhole connecting the servo arm to the strut. The analytical analysis revealed the maximum stress in the part as 23.7 MPa, meanwhile the numerical solution based on a finite element model (FEM) converged towards a lower stress result of 22.8 MPa, as seen in Figure 8.

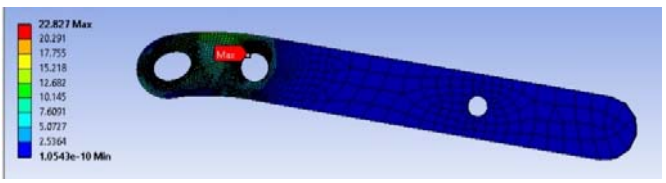

Figure 9 - FEM model stress result

The coinciding results indicate a valid FEM analysis and stress result. The factor of safety for a break with the drone

perching from the cable was found to be 1.25 by comparing the result to the 3D print filament material strengths.

Further considerations for future designs include protection of the core and coil parts and simplifying the mechanism and drivetrain to achieve higher efficiency (lower consumption) and lower total mass.

CONCLUSION

The work aims to evaluate the feasibility of a charging function for drones on overhead power lines and to verify this in a test setup. For practical application, the available power in relation to the current in the overhead line and the additional weight of the Energy Harvester for the drone is the main parameter to be determined.

According to initial considerations and theoretical calculations, the available power at typical currents and a reasonable weight of the harvester with over 100 W are within a useful range. The difficulty lies in practical implementation. The key component is the material of the transformer core. At the high field strengths and relatively high power levels, a saturation effect occurs early on, which leads to a significant reduction in the available power. The solution has therefore not yet reached the limit of its suitability. Therefore, a further investigation of the new materials is planned in the following work.

The safety factor for a break in the mechanical mechanism was determined too low and the part was a subject for future material change or geometry optimization. It was furthermore determined to re-design the mechanism with a focus on improving the previously mentioned areas.

REFERENCES

[1] Project web-page “Drones4Energy” https://drones4energy.dk/

[2] G. Mehrooz, E. Ebeid, P. Schneider-Kamp, „System Design of an Open-Source Cloud-Based Framework for Internet of Drones Applications”, Proceedings of conference Euromicro Digital System Design, 2019

[3] L. Shi, N.-J. Hernández Marcano, R. Jacobsen, “A Survey on Multi-Unmanned Aerial Vehicle Communications for Autonomous Inspections”, Euromicro Digital System Design, 2019

[4] J. Dai, D. C. Ludois, “A Survey of Wireless Power Transfer and a CriticalComparison of Inductive and Capacitive Couplingfor Small Gap Applications”, IEEE TRANSACTIONS ON POWER ELECTRONICS, VOL. 30, NO. 11, NOVEMBER 2015

[5] X. Lu, P. Wang, D. Niyato, D. I. Kim, Z. Han, „Wireless Charging Technologies: Fundamentals, Standards, and Network Applications”, IEEE COMMUNICATIONS SURVEYS & TUTORIALS, VOL. 18, NO. 2, SECOND QUARTER 2016

[6] C. H. Choi et al, “Automatic Wireless Drone Charging Station”, International Conference on Control, Automation and Information Sciences (ICCAIS), Ansan, Korea, 2016

[7] A. Hennig, P. Gembaczka, L. Cousin, A. Grabmaier, “Smart Self-Sufficient Wireless Current Sensor”, European Conference on Smart Objects, Systems and Technologies, Dresden, GERMANY 2018

[8] F. U. Khan, “Energy Harvesting from the Stray Electromagnetic Field around the Electrical Power Cable for Smart Grid Applications”, Hindawi Publishing Corporation. The Scientific World Journal Volume, 2016, Article ID 3934289, 20 pages

[9] SG-Transmission, Electromagnet datasheet (Online: 07-05-2020) https://www.sgtransmission.com/wp-content/uploads/2014/10/Electromagnet-Type-58-V2.pdf